



HAL
open science

Insight into the Modes of Activation of Pyridinium and Bipyridinium Salts in Non-Covalent Organocatalysis

Robin Weiss, Tamara Golisano, Patrick Pale, Victor Mamane

► **To cite this version:**

Robin Weiss, Tamara Golisano, Patrick Pale, Victor Mamane. Insight into the Modes of Activation of Pyridinium and Bipyridinium Salts in Non-Covalent Organocatalysis. *Advanced Synthesis and Catalysis*, In press, 10.1002/adsc.202100865 . hal-03331312

HAL Id: hal-03331312

<https://hal.science/hal-03331312v1>

Submitted on 1 Sep 2021

HAL is a multi-disciplinary open access archive for the deposit and dissemination of scientific research documents, whether they are published or not. The documents may come from teaching and research institutions in France or abroad, or from public or private research centers.

L'archive ouverte pluridisciplinaire **HAL**, est destinée au dépôt et à la diffusion de documents scientifiques de niveau recherche, publiés ou non, émanant des établissements d'enseignement et de recherche français ou étrangers, des laboratoires publics ou privés.

Insight into the Modes of Activation of Pyridinium and Bipyridinium Salts in Non-Covalent Organocatalysis

Robin Weiss,^a Tamara Golisano,^a Patrick Pale,^a and Victor Mamane^{a*}

^a Dr. R. Weiss, T. Golisano, Prof. Dr. P. Pale, Dr. V. Mamane
Institute of Chemistry of Strasbourg, UMR 7177 - LASYROC
CNRS and Strasbourg University
4 rue Blaise Pascal, 67000 Strasbourg, France
E-mail: vmamane@unistra.fr (VM)

Received:



Supporting information for this article is available on the WWW

Abstract. A series of pyridinium and bipyridinium salts were prepared and their catalytic properties were evaluated in the aza-Diels-Alder between imines and Danishefsky diene. Depending on the substituents of the pyridinium/bipyridinium rings and on the nature of the counter-anion, two mechanisms of activation were demonstrated. In case of non-substituted rings, the substrate is activated through charge transfer involving the aryl ring on the C-side of the imine. When halogen atoms were introduced on the catalysts, the activation mode switched to halogen bond involving the imine nitrogen lone pair. Moreover, alternative activation modes based on hydrogen bonding and radical cation were ruled out.

This work allowed us to develop two families of catalysts whose potential was demonstrated in the cycloaddition of various imines with Danishefsky diene. The first family is composed of the simple methyl pyridinium triflate and dioctyl bipyridinium triflate. The former is active only with imines bearing a *p*-methoxyphenyl group on the C-side and the latter was found to be efficient with imines bearing different substituents on both the N- and C-sides of the imines. The second family is based on halogenated pyridinium salts which proved active with almost all considered imines.

Keywords: Charge transfer; Halogen bond; Organocatalysis; Hetero Diels-Alder; Pyridinium

Introduction

N-Substituted pyridinium salts are privileged structural units of significant importance in natural products and synthetic chemistry.^[1] This scaffold is found in the nicotinamide adenine dinucleotide (NAD⁺) cofactor essential to all organisms^[2] and in some marine sponges^[3] (Figure 1, top). Besides, pyridinium salts can serve as functional group transfer reagents,^[4] phase-transfer catalysts^[5] and ionic liquids.^[6] Pyridinium salts have also been widely used as synthetic intermediates, for example in ring opening cascade reactions and dienal formation,^[7] 1,3-dipolar additions^[8] and photochemical transformations^[9] (Figure 1, middle). In contrast, *N,N'*-disubstituted bipyridinium salts were far less studied. Although a few bipyridiniums have been proposed as antibacterial,^[10] (Figure 1, bottom), the main application of bipyridinium salts is as functional materials, with viologen as archetypal compound.^[11]

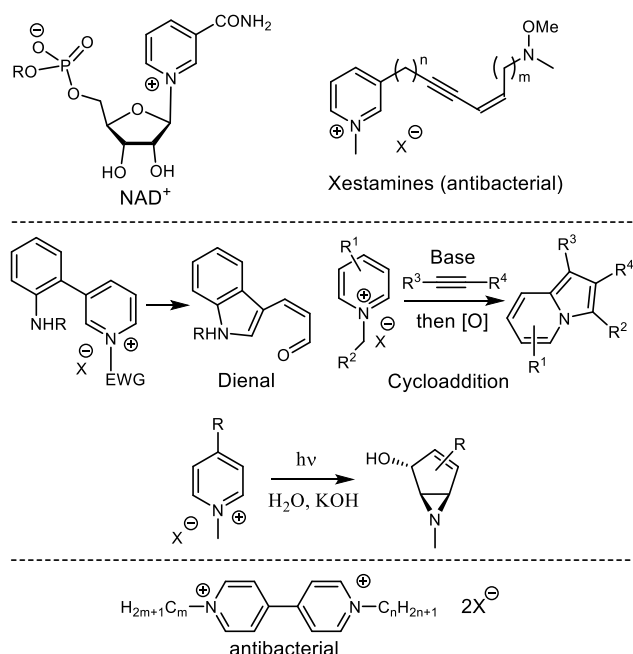


Figure 1. Pyridinium and bipyridinium salts: selected natural products and applications.

However, the use of pyridinium and bipyridinium salts in organocatalysis is very limited. Indeed, only a handful of examples report the application of pyridiniums and even less of bipyridinium as catalyst. Surprisingly, different modes of action have been proposed for these catalysts, depending on the nature of the substituents on the heterocycle and the considered reaction (Figure 2). Deciphering the exact mechanism is not always straightforward, and represents a real challenge, not addressed so far.

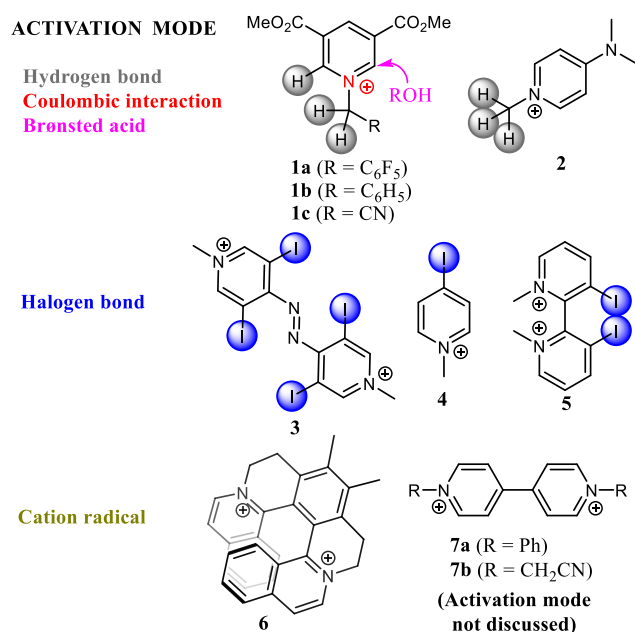


Figure 2. Pyridinium and bipyridinium salts in organocatalysis and their proposed mode of activation (counterions are not shown for clarity).

Berkessel proposed that catalyst **1a** dissociates 1-chloroisochroman *via* Coulombic interaction with chloride, thus allowing Mukaiyama aldol-type reaction with silyl ether nucleophiles.^[12] Later, on the basis of X-ray data of **1a** with halide counteranions (Cl⁻ and Br⁻), Nagorny and Sun suggested that **1a** could also act as hydrogen bond (HB) donor.^[13] Activation through HB was also proposed by Bibal with catalyst **2** in the ring-opening polymerization of cyclic esters^[14] and for aminolysis of epoxides.^[15] However, in these cases, catalyst **2** was used in combination with two co-catalysts, rendering any interpretation less clear. With catalysts of type **1** bearing a phenyl (**1b**) or cyano group (**1c**), a mechanism based on alcohol addition to the catalyst and generation of a Brønsted acid was proposed by Connon for the acetalization of aldehydes and ketones^[16] and by Berkessel for the addition of alcohols to glycals.^[17] When iodine atom is introduced on the charged heterocycle, activation via halogen bond (XB)-based could operate.^[18] Indeed, iodine

electrophilicity, which is directly related to its σ -hole depth,^[19] is increased due to the positive charge of the pyridinium heterocycle; iodine thus acts as a Lewis acid.^[20] Although not used as a catalyst, compound **3** developed by Huber was the first iodo-bipyridinium able to promote the Ritter reaction through XB activation of benzhydryl bromide.^[21] More recently, Yeung described that 4-iodopyridinium **4** was able to catalyse the intramolecular bromocarbocyclization of cinnamyl ethers and sulfonamides through XB activation of *N,N*-dibromodimethylhydantoin.^[22] In 2020, Toy reported that bipyridinium **5** was a more efficient XB catalyst than its monomeric 3-iodopyridinium analogue in Friedel-Crafts reaction with furans.^[23] Pospíšil demonstrated that pyridinium- and isoquinolinium-based helquats **6** could catalyse Povarov reaction through a cation radical mechanism.^[24] Mayer used bipyridiniums **7a,b** as catalysts in imine aziridination and Povarov reaction,^[25] but their mode of activation was not discussed.

Herein, in continuation to our efforts to develop efficient XB and related chalcogen bond donors for catalysis applications,^[26] new polyhalogenated pyridinium and bipyridinium salts were designed to face/address the above mentioned challenge (Figure 2) and to gain real clues on their mode of action (Figure 3). To study the catalytic activity of these (bi)pyridinium salts, we selected the aza-Diels-Alder^[27] reaction between Danishefsky's diene and imines. In the literature, the aza-Diels-Alder reaction between Danishefsky's diene and imines was shown to be catalysed through HB with tetraalkylammonium^[28] and trialkylsulfonium^[29] salts and through XB with iodotriazolium or iodoimidazolium salts.^[30] Recently, through theoretical calculations, the role of Coulombic (dipole-cation) interactions was also highlighted with onium catalysts.^[31] Therefore, the polyhalogenated (bi)pyridinium salts reported here can in principle activate a substrate through the different modes of activation depicted in Figure 2.

We demonstrated here that Coulombic interactions are operative with naked heterocycles, whereas XB is the principal mode of activation when the heterocycles bear multiple halogens (Figure 3). Interestingly, HB is not operative with this class of compounds despite the acidity of the pyridinium hydrogens.

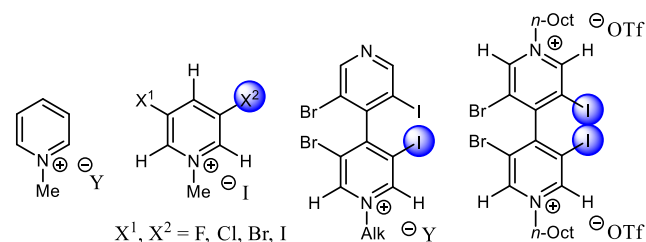
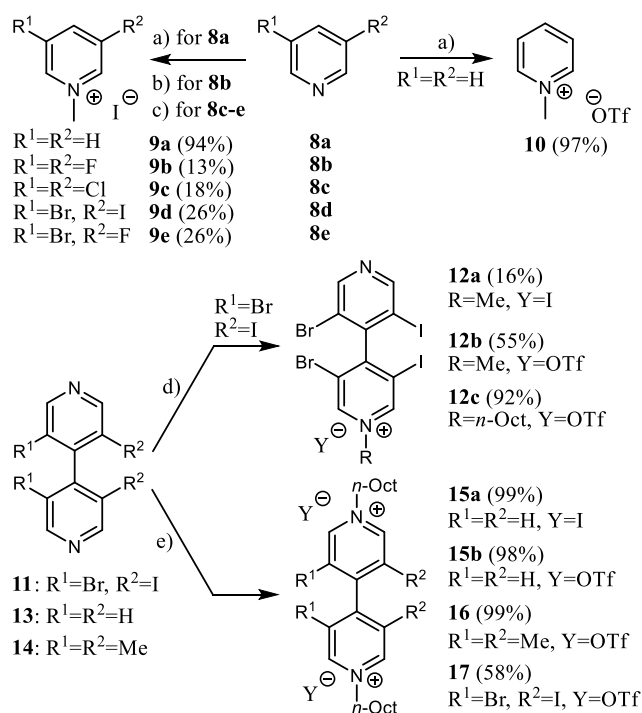


Figure 3. Pyridinium and bipyridinium salts considered in this study (Y = I or OTf).

Results and Discussion

N-Alkyl pyridinium and bipyridinium salts were prepared by alkylation of their parent pyridines and 4,4'-bipyridines. Thus, addition of methyl iodide to the commercially available pyridines **8a-c** and **8e** as well as to **8d**, obtained from the commercial 3,5-dibromopyridine, furnished the iodide salts **9a-e**. Analogously, pyridine **8a** was reacted with methyl triflate to produce the *N*-methyl pyridinium triflate **10**. Mono-alkylation of 4,4'-bipyridine **11**^[32] with respectively methyl iodide, methyl triflate and octyl triflate delivered the iodide salt **12a** and the triflate salts **12b,c**. Finally, the double alkylation of 4,4'-bipyridines **11**, **13** and **14**^[33] gave the bis-*N*-octyl-bipyridinium triflates **15a**, **15b**, **16** and **17**, respectively (Scheme 1).



Scheme 1. Synthesis of pyridinium and bipyridinium salts. a) CH_3I or CH_3OTf (2 eq.), CH_3CN , MW 300W, $120^\circ C$, 2h; b) CH_3I (1.35 eq.), Et_2O , MW 300W, $50^\circ C$, 1h; c) CH_3I (4 eq.), Et_2O , $25^\circ C$, 24h; d) **12a**: CH_3I (1 eq.), CH_3CN , $70^\circ C$, 48h; **12b**: CH_3OTf (1 eq.), Et_2O , $25^\circ C$, 24h; **12c**: *n*-OctOTf (1 eq.), Et_2O , $25^\circ C$, 24h; e) **15a**: *n*-OctI (4 eq.), CH_3CN , $120^\circ C$, 24h; **15b** and **16**: *n*-OctOTf (4 eq.), CH_3CN , $120^\circ C$, 24h; **17**: *n*-OctOTf (4 eq.), CH_3CN , $25^\circ C$, 24h.

The pyridinium and bipyridinium salt were tested in the reaction between Danishefsky's diene **18** and imines **19a-b** in dichloromethane at room temperature (Table 1).

No reaction occurred without catalyst after 24h (entries 1 and 2) as well as with iodide **9a**, even after addition of acetonitrile in order to increase its solubility (entries 3 and 4). Rewardingly, the reaction was complete within 5 min with 5 mol% of triflate **10** and the cyclized product **20a** was quantitatively formed (entry 5). Complete conversion was also obtained by addition of K_2CO_3 in the reaction mixture

containing catalyst **10**; this result thus ruled out the possible role of hidden Brønsted acid (entry 6). A radical mechanism was also excluded by performing the reaction in the presence of butylated hydroxytoluene (BHT) with no change in the yield (entry 7). Moreover, tetrabutylammonium triflate (TBAOTf) was inactive in the reaction (entry 8); this interesting result showed that the triflate anion did not play a role in the catalytic activity of **10**, but also that HB-catalysis driven by ammonium chains^[28] was not operative under such conditions.

These first series of experiments suggests that dipole-cation interaction^[31] or even charge transfer could be responsible for reaction initiation, but not HB. The inactivity of the iodide salt **9a** could be due to the charge transfer occurring between the pyridinium and iodide, which do not allow the imine substrate to interact with the catalyst. In contrast, in the triflate salt **10**, the interaction of the triflate anion with the charged heterocycle is weaker, the latter could thus be able to activate the substrate through charge transfer facilitated by the presence of a *p*-methoxy group in **19a**. To check this hypothesis, the imine substrate was switched from **19a** ($R = OMe$) to **19b** ($R = Me$). Rewardingly, the reaction was completely inhibited with this substrate, and no formation of the cyclized product **20b** could be observed (entry 9). Charge transfer seems thus responsible for the activity of catalyst **10**.

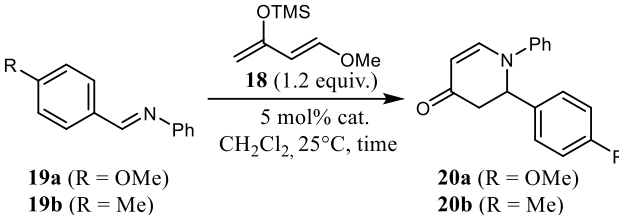
In a second series of experiments (entries 10-13), halogenated pyridinium iodides **9b-e** were used as catalysts (5 mol%) in the aza-Diels-Alder reaction involving imine **19a** in order to evaluate the possible implication of HB and/or XB modes of activation with these catalysts. In iodides salts **9b-e**, two halogen atoms acting as electron-withdrawing substituents were added in 3- and 5-positions of **9a**, thus increasing the acidity of the hydrogen atoms in 2- and 2'-positions. Moreover, the σ -hole of these halogens is deepened because of the positive charge, except for fluorine whose σ -hole is rarely positive.

Pyridinium **9b** bearing two fluorine atoms was completely inactive in the reaction despite the presence of acidic hydrogens, ruling out HB role (entry 10). A low yield of 40% was observed with **9c** bearing chlorines as potential XB sites (entry 11). With pyridiniums **9d** and **9e** bearing bromine and iodine as XB donors, the yields reached about 60% (entries 12 and 13). In this series, the reactivity clearly increased with the σ -hole intensity of the halogen whereas it decreased with the hydrogen acidity. It is then likely that pyridiniums iodides **9c-e** catalyze the reaction through XB activation of the imine substrate.

With the aim to further increase iodine σ -hole, pyridiniums **12** bearing an additional electron-withdrawing group in 4-position (3-bromo-5-iodo-4-pyridinyl) compared to **9d**, were prepared and evaluated as catalyst. Gratifyingly, the catalytic activity of these pyridiniums was greatly enhanced and in all cases, high to quantitative yields were obtained after only 5 min. Interestingly, shifting from iodide **12a** to triflate **12b** as catalyst increased reaction yields

(77 vs 87%, respectively; entries 14 vs 15) as expected from stronger XB interaction of iodide compared to triflate. Quantitative yield was obtained with the more soluble *N*-octyl pyridinium triflate **12c** after 5 min (entry 16). Interestingly, the same result was obtained when using imine **19b** (entry 17).

Table 1. Aza-Diels-Alder Reaction Catalysed by Pyridinium salts.



Entry	Imine	Catalyst	Additive ^{a)}	Time	Yield (%) ^{c)}
1	19a (R = OMe)	None	-	24h	0
2	19a (R = OMe)	None	- ^{b)}	24h	0
3	19a (R = OMe)	9a	-	24h	0
4	19a (R = OMe)	9a	- ^{b)}	24h	0
5	19a (R = OMe)	10	-	5min	99
6	19a (R = OMe)	10	1 eq. K ₂ CO ₃	1h	99
7	19a (R = OMe)	10	0.05 eq. BHT	1h	99
8	19a (R = OMe)	TBAOTf	-	1h	0
9	19b (R = Me)	10	-	1h	0
10	19a (R = OMe)	9b	- ^{b)}	1h	0
11	19a (R = OMe)	9c	- ^{b)}	1h	40
12	19a (R = OMe)	9d	- ^{b)}	1h	55
13	19a (R = OMe)	9e	- ^{b)}	1h	60
14	19a (R = OMe)	12a	-	5min	77
15	19a (R = OMe)	12b	-	5min	84
16	19a (R = OMe)	12c	-	5min	99
17	19b (R = Me)	12c	-	5min	99
18	19a (R = OMe)	12c	0.1 eq. TBACl	5min	38
19	19a (R = OMe)	12c	0.2 eq. TBACl	5min	0
20	19a (R = OMe)	15a	-	1h	0
21	19a (R = OMe)	15b	-	5min	99
22	19a (R = OMe)	15b	1 eq. K ₂ CO ₃	5min	99
23	19a (R = OMe)	15b	0.05 eq. BHT	5min	99
24	19b (R = Me)	15b	-	1h	99
25	19a (R = OMe)	16	-	1h	0
26	19a (R = OMe)	17	-	5min	87
27	19b (R = Me)	17	-	5min	90
28	19a (R = OMe)	17	0.2 eq. TBACl	5min	0

Conditions: Imine **19a** or **19b** (0.14 mmol), diene **18** (0.17 mmol), in ^{a)} CH₂Cl₂ or ^{b)} CH₂Cl₂/CH₃CN 9/1 (2 mL), hexamethylbenzene as internal standard (78 μL of a 0.1 M solution in CH₂Cl₂); ^{c)} Determined by ¹H NMR.

To confirm that halogen bonding is involved, we performed competitive experiments in the presence of

tetrabutylammonium chloride (TBACl). As chloride anion is known to act as good σ -hole acceptor,^[34] it can interact through XB with the σ -hole carried by the catalyst halogen(s) and thus compete with the substrate. This competition should lower the catalyst efficacy.^[30b] With imine **19a**, the catalytic activity of **12c** was indeed lowered by addition of 10 mol% of TBACl (2 equiv. with regard to **12c**) (entry 18) and completely suppressed with 20 mol% of TBACl (4 equiv. with regard to **12c**) (entry 19). It is worth noting that after addition of the two first equivalents of chloride anion, the residual catalytic activity (38%) was probably due to the XB with the remaining halogens on the pyridine ring, as it is suppressed when one chloride per halogen was added (entry 19 vs 18 vs 17).

These set of results of this third series of experiments (entries 14-19) clearly suggest that the reaction is catalyzed through XB with pyridinium **12a-c**.

In order to have more insight on this XB mode of activation, crystals of pyridiniums **12a** and **12b** were grown and their solid-state structures were analyzed by X-ray diffraction (Figure 4).

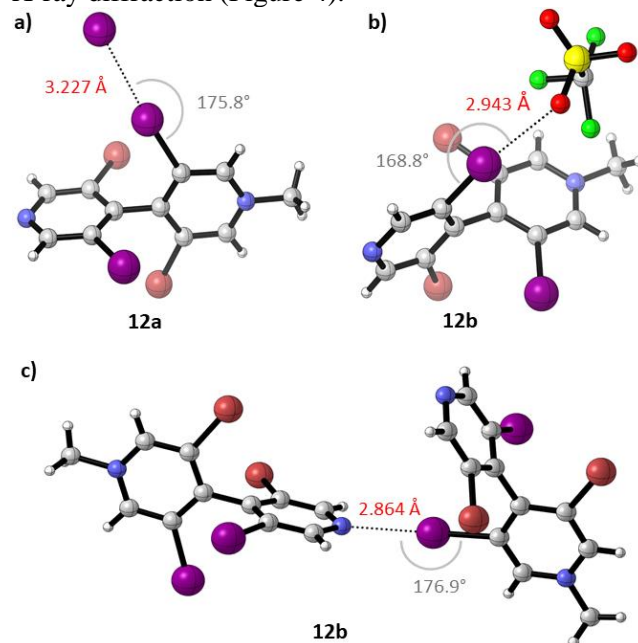


Figure 4. X-Ray structures of pyridiniums **12a** (a) and **12b** (b and c) using CYLView.^[35] Color code: carbon in grey, hydrogen in white, bromine in orange, iodine in violet, nitrogen in blue, oxygen in red, sulphur in yellow and fluorine in green.

In the structure of **12a** (Figure 4a), as expected, a XB was observed between the iodine on the pyridinium cycle and the iodide anion through a strong interaction revealed by a I...I distance (3.327 Å) well below the sum of the van der Waals radii (I 1.98 Å), and with a C-I...I angle of 175.8°. The iodide is probably a competitor in the reaction, thus explaining the lower activity of **12a** compared to **12b**.

In the structure of **12b**, the triflate anion is also interacting through XB but with the pyridinyl iodine (Figure 4b). Interestingly, a strong XB was observed between the iodine on the pyridinium cycle and the pyridine nitrogen of another unit (N---I 2.864 Å and N---C-I 176.9°) (Figure 4c). These data suggest that the pyridine nitrogen should be replaced in solution by the imine nitrogen in the XB observed in solid state. They also indicate that triflate **12b** should better activate the imine substrate through XB than **12a**, as observed.

Finally, in order to confirm the charge transfer or XB modes of activation of naked *vs* halogenated heterocycles, the bipyridinium salts **15-17** were also evaluated as catalysts in the same aza-Diels-Alder reaction.

As with the simple pyridiniums **9a** and **10**, the bipyridinium bis iodide **15a** was inactive (entry 20) whereas the bis triflate salt **15b** was (entry 21). The latter showed higher activity compared to pyridinium triflate **10** since complete conversion was obtained after only 5 min at room temperature (entry 21 *vs* 5). Here again, hidden Brønsted acid (entry 22) and involvement of radical mechanism were ruled out (entry 23).

In contrast to its monomeric counterpart **10** (entry 9), bipyridinium **15b** was able to activate imine **19b** to generate the cyclized product quantitatively after 1h of reaction (entry 24 *vs* 9). This result could easily be explained by better charge transfer due to the structural analogy of **15b** to viologen. As for charge transfer, the formation of a complex through π -orbital interaction is required before charge transfer, we designed the 3,3',5,5'-tetramethylbipyridinium **16** in order to look at conformational effect on the catalytic activity.

Interestingly, reaction with imine **19a** was completely suppressed by using **16** as catalyst (entry 25). The methyl groups in **16** thus prevent charge transfer between the pyridinium ring and the imine, probably by inducing the non-planarity of the two pyridinium moiety and/or by hindering each side of the pyridinium plane. When the methyl groups were replaced by halogens such as in **17**, reaction occurred again and high yields were obtained for both imines **19a-b** (entries 26 and 27), although these yields were slightly lower compared to the ones achieved with the pyridinium analogue **12c** (entries 16 and 17). The role of XB in the activation of imines **19a-b** by **17** was confirmed by TBACl addition which resulted in complete inactivation of the catalyst (entry 28).

To sum up, non-substituted pyridinium and bipyridinium triflates **10** and **15b** activate imine substrates through Coulombic interaction and charge transfer^[31] (Fig. 5a), whereas the halogenated ones, **9b-c**, **12b-c** and **17**, are operating through XB (Fig. 5c). Activation through charge transfer could be inhibited by steric constrains (Fig. 5b).

After having demonstrated that pyridinium and bipyridinium act as catalysts in aza-Diels-Alder reaction and elucidated their respective modes of action, the reaction scope was studied by using different imines in the presence of 5 mol% of catalyst

10, **12c** and/or **15b**. For comparison purposes, all reactions were performed with Danishefsky's diene **18** over 1h (Table 2).

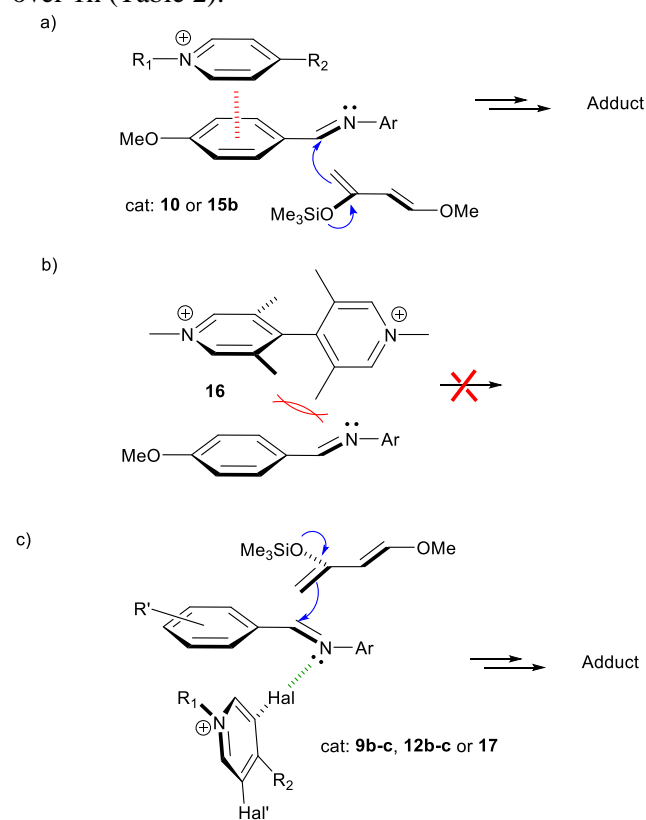
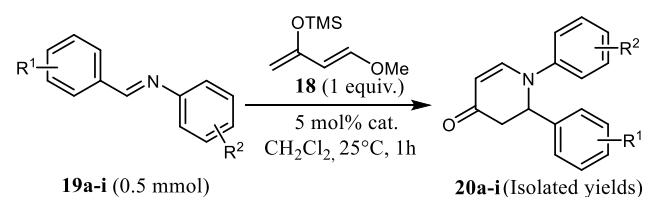
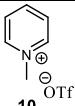
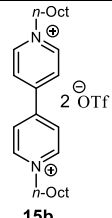
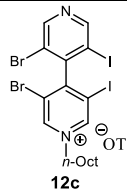
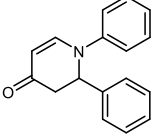
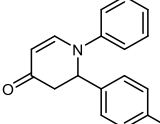
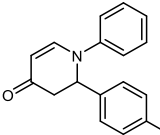
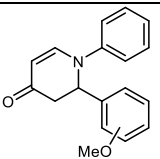
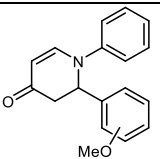
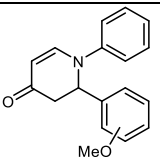
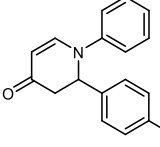
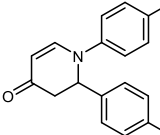
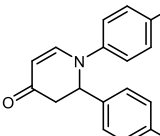


Figure 5. Schematized modes of activation of pyridinium organocatalysts: Activation by Coulombic interaction and charge transfer (a) or by halogen bond (b); inhibition of charge transfer due to steric constrains (c).

The halogenated pyridinium **12c** could efficiently catalyze the reaction of almost all considered imines with yields comprised between 72 and 91%, except for imine **19g** bearing a *p*-dimethylamino group. The latter could not be converted to **20g**, even after 18h of reaction and in the presence of 10 mol% of catalyst. In this case, the XB-driven catalyst is probably deactivated by the good XB acceptor ability of the dimethylamino group. As expected from this XB activation mode, a slight electronic effect could be observed with imines carrying electron-withdrawing substituent on the aryl group. Imines **19c** and **19e** were slightly less efficiently converted with catalyst **12c** to adducts **20c** and **20e** than other imines (72-76% *vs* 82-93%).

Table 2. Scope of the charge-transfer or XB-catalyzed aza-Diels-Alder reaction.



			
 20a	-	95%	93%
 20b	0	93%	90%
 20c	0	71%	76%
 <i>ortho</i> 20d	0	65%	91%
 <i>meta</i> 20e	0	61%	72%
 <i>para</i> 20f	77%	85%	82%
 20g	0	70%	0
 20h	10%	-	84%
 20i	92%	-	89%

With pyridinium **10**, as expected from the screening above, only imines **19a** and **19i** bearing *p*-methoxyphenyl substituent could be cyclized giving products **20a** and **20i** in good yields. A low yield of **20h** was obtained with imine **19h** containing the *p*-methoxyphenyl substituent on the nitrogen.

In contrast, the bipyridinium catalyst **15b** readily catalyzed the reaction of all the imines tested **19a-g**, the expected adducts **20a-g** were always produced in good to high yields (61-95%). These results revealed the significant reactivity increase of the bipyridinium catalyst **15b** compared to its simple pyridinium analog **10**. Nevertheless, and as expected from the mode of action established above, electronic and steric effects affect the reaction outcome. Imines **19d-e** bearing a methoxy substituent respectively in *ortho* and *meta* positions were cyclized with lower yields, and the

cyclization of the dimethylamino-substituted imine **19g** required higher catalyst loading (10 mol%) and prolonged reaction time (18h) to achieve a good yield of **20g**.

Conclusion

A series of halogenated and non-halogenated pyridinium and bipyridinium catalysts were designed to explore the various activation modes in the organocatalyzed reaction of imines with Danishefsky's diene. The gained results allowed to discriminate the mode of activation of this family of catalysts with imine substrates. It was clearly demonstrated that non-halogenated derivatives activate the imine through charge transfer whereas the halogenated ones interact with the imine nitrogen through XB. Besides methyl pyridinium triflate catalyst (**10**) which showed good performance only with imines having a *p*-methoxyphenyl substituent on the imine carbon side, two powerful catalysts **12c** and **15b** based on the 4,4'-bipyridine scaffold were developed during this work. Further work is now underway in our laboratory in order to expand the scope of reactions that can be catalyzed by these molecules.

Experimental Section

General methods. Et₂O was distilled over Na/benzophenone and freshly used. CH₂Cl₂ and CH₃CN were dried by passing through activated alumina under a positive pressure of argon using GlassTechnology GTS100 devices. Anhydrous reactions were carried out in flame-dried glassware and under an argon atmosphere, using standard Schlenk techniques. Column chromatography was performed with silica gel from Merck (Kieselgel 60; 63-200 μm or 40-63 μm). ¹H, ¹³C and ¹⁹F NMR spectra were recorded on Bruker Advance 300, 400 or 500 spectrometers. Chemical shifts were determined by taking the solvent as a reference. Mass spectrometry (HRMS) experiments were performed on a Bruker Daltonics microTOF spectrometer (Bruker Daltonik GmbH, Bremen, Germany) by the Service de Spectrométrie de Masse de la Fédération de Chimie "Le Bel" (FR 2010). Pyridines **8a-c**, **8e** and bipyridine **13** were purchased and used as received.

3-bromo-5-iodopyridine (8d). To a solution of 3-5 dibromo-pyridine (10.8 mmol, 2.60 g) in THF (50 mL), was added a solution of *i*PrMgCl·LiCl (11.8 mmol, 1.3 M in THF, 9.1 mL) at -10 °C. After 10 min of stirring a solution of iodine (11.8 mmol) in THF (16 mL) was added dropwise, keeping the temperature below -5 °C. After 10 min of stirring Et₂O (200 mL) was added and was washed with NaHSO₃ sat. (60 mL). Organic extract was washed with brine (100 mL), dried over Na₂SO₄, filtered, and concentrated to give the desired product without further necessary purification. (3.05 g, 99% yield). White solid. ¹H NMR (600 MHz, Chloroform-*d*) δ 8.74 (dd, *J* = 1.8, 0.5 Hz, 1H), 8.62 (dd, *J* = 2.1, 0.5 Hz, 1H), 8.18 – 8.13 (m, 1H).

General procedure for the synthesis of 9a and 10. Pyridine (0.5 mmol, 40 mg) was solubilized in CH₃CN (2 mL) and placed in a specific microwave tube equipped with a magnetic stir bar, then was added the electrophile RX (1 mmol). The tube was placed in the microwave cavity (CEM Discover) and submitted to irradiation for 2 h at 120 °C using a maximum power of 300 W. After cooling to room temperature, the mixture was concentrated, Et₂O (10 mL)

was added and the suspension was filtrated, washed with Et₂O (2 x 5 mL) and dried under vacuum overnight to give the desired product.

1-Methylpyridin-1-ium iodide (9a).^[36] Yellow solid; 100 mg, yield: 94%. ¹H NMR (500 MHz, DMSO-*d*₆) δ 9.01 (d, *J* = 6.1 Hz, 2H), 8.59 (t, *J* = 7.8 Hz, 1H), 8.14 (t, *J* = 7.1 Hz, 2H), 4.37 (s, 3H); ¹³C NMR (126 MHz, DMSO-*d*₆) δ 145.4, 145.0, 127.6, 48.0.

1-Methylpyridin-1-ium trifluoromethanesulfonate (10).^[37] White solid; 120 mg, yield: 97%. ¹H NMR (400 MHz, CD₃CN) δ 8.66 (d, *J* = 5.2 Hz, 2H), 8.49 (t, *J* = 7.9 Hz, 1H), 8.04-7.96 (m, 2H), 4.31 (s, 3H); ¹⁹F NMR (282 MHz, CD₃CN) δ -78.16 (s, 3F).

3,5-Difluoro-1-methylpyridin-1-ium iodide (9b).^[38] 3,5-Difluoropyridine (2.7 mmol, 310 mg) was solubilized in Et₂O (4 mL) and placed in a specific microwave tube equipped with a magnetic stir bar, then was added the electrophile CH₃I (3.6 mmol, 0.51 g). The tube was placed in the microwave cavity (CEM Discover) and submitted to irradiation for 1 h at 50 °C using a maximum power of 300 W. After cooling to room temperature, Et₂O (30 mL) was added and the suspension was filtrated, washed with Et₂O (2 x 15 mL) and dried under vacuum overnight to give the desired product (90 mg, 13% yield). Yellow solid. ¹H NMR (500 MHz, CDCl₃) δ 9.26-9.11 (m, 2H), 8.71 (t, *J* = 8.3 Hz, 1H), 4.49 (s, 5H); ¹³C NMR (126 MHz, CD₃OD) δ 162.1 (dd, *J* = 257.1, 12.3 Hz), 134.7, 123.3-122.2 (m), 50.2; ¹⁹F NMR (471 MHz, CDCl₃) δ -111.00 (t, *J* = 125.5 Hz).

General procedure for the synthesis of 9c-9e. Halogenated pyridine (1 eq.) was solubilized in a Et₂O (2 mL) and placed in a tube equipped with a magnetic stir bar. CH₃I (4 eq.) was added and the tube was sealed with a screw cap. The mixture was stirred for 24 h at 25 °C. Then, the mixture was filtrated and washed with Et₂O (2 x 5 mL) and dried under vacuum overnight to give the desired product.

3,5-Dichloro-1-methylpyridin-1-ium iodide (9c). Starting from 3,5-dichloropyridine (0.20 g, 1.3 mmol) and CH₃I (0.77 g, 5.4 mmol). 68 mg, yield: 18%. White solid, mp 204-206 °C; ¹H NMR (500 MHz, CD₃OD) δ 9.26 (d, *J* = 1.9 Hz, 2H), 8.93 (t, *J* = 1.9 Hz, 1H), 4.43 (s, 4H); ¹³C NMR (126 MHz, CD₃OD) δ 144.7, 144.0, 135.4, 48.3; HRMS (ESI-TOF) *m/z* calcd for C₆H₆Cl₂N: 161.9871 [M]⁺; found, 161.9879; *m/z* calcd for I: 126.9042 [M]⁺; found, 126.9050.

3-Bromo-5-iodo-1-methylpyridin-1-ium iodide (9d). Starting from 3-bromo-5-iodopyridine (0.20 g, 0.70 mmol) and CH₃I (0.17 g, 2.8 mmol). 78 mg, yield: 26%. Yellow solid, mp 188-190 °C; ¹H NMR (500 MHz, D₂O) δ 9.09 (s, 1H), 9.04 (s, 1H), 9.02 (s, 1H), 4.23 (s, 3H); ¹³C NMR (126 MHz, D₂O) δ 155.5, 149.8, 145.5, 122.1, 92.9, 48.1; HRMS (ESI-TOF) *m/z* calcd for C₆H₆BrIN: 297.8723 [M]⁺; found, 297.8730; *m/z* calcd for I: 126.9041 [M]⁺; found, 126.9050.

3-Bromo-5-fluoro-1-methylpyridin-1-ium iodide (9e). Starting from 3-bromo-5-fluoropyridine (0.20 g, 1.14 mmol) and CH₃I (0.64 g, 4.55 mmol). 96 mg, yield: 26%. Yellow solid, mp 215-218 °C; ¹H NMR (500 MHz, Methanol-*d*₄) δ 9.39 - 9.13 (m, 2H), 8.97 - 8.89 (m, 1H), 4.45 (s, 3H); ¹³C NMR (126 MHz, Methanol-*d*₄) δ 161.3 (d, *J* = 258.4 Hz), 145.9, 137.2 (d, *J* = 21.3 Hz), 136.7 - 135.9 (m), 124.2, 49.8; HRMS (ESI-TOF) *m/z* calcd for C₆H₆BrFN: 189.9662 [M]⁺; found, 189.9654; *m/z* calcd for I: 126.9038 [M]⁺; found, 126.9050.

3,3'-Dibromo-5,5'-diiodo-1-methyl-[4,4'-bipyridin]-1-ium iodide (12a). Bipyridine **11** (60 mg, 0.11 mmol) was solubilized in CH₃CN (2 mL) and placed in a tube equipped with a magnetic stir bar. CH₃I (16 mg, 0.11 mmol) was added and the tube was sealed with a screw cap. The mixture was stirred for 48 h at 70 °C. After cooling to room temperature, the mixture was filtrated and washed with Et₂O (2 x 5 mL) and dried under vacuum overnight to give the

desired product. 12 mg, yield: 16%. Orange solid, mp 230-234 °C; ¹H NMR (500 MHz, DMSO-*d*₆) δ 9.74 (s, 1H), 9.72 (s, 1H), 9.20 (s, 1H), 9.06 (s, 1H), 4.37 (s, 3H); ¹³C NMR (126 MHz, DMSO-*d*₆) δ 159.3, 156.5, 152.4, 151.4, 150.6, 148.0, 120.9, 114.8, 99.8, 96.7, 48.3; HRMS (ESI-TOF) *m/z* calcd for C₁₁H₇Br₂I₂N₂: 578.7060 [M]⁺; found, 578.7091; *m/z* calcd for I: 126.9050 [M]⁺; found, 126.9042.

General procedure for the synthesis of 12b-12c. Bipyridine **11** (1 eq.) was solubilized in a Et₂O (2 mL) and placed in a tube equipped with a magnetic stir bar. CH₃OTf or *n*-Octyl-OTf (1 eq.) was added and the tube was sealed with a screw cap. The mixture was stirred for 24 h at 25 °C. Then, the mixture was filtrated and washed with Et₂O (2 x 5 mL) and dried under vacuum overnight to give the desired product.

3,3'-Dibromo-5,5'-diiodo-1-methyl-[4,4'-bipyridin]-1-ium trifluoromethanesulfonate (12b). Starting from bipyridine **11** (100 mg, 0.18 mmol) and methyltriflate (28 mg, 0.18 mmol). 72 mg, yield: 55%. White solid, mp 183-185 °C; ¹H NMR (300 MHz, Acetone-*d*₆) δ 9.88-9.82 (m, 1H), 9.80-9.77 (m, 1H), 9.22 (s, 1H), 9.04 (s, 1H), 4.75 (s, 3H); ¹³C NMR (126 MHz, Acetone-*d*₆) δ 161.3, 157.5, 154.0, 152.4, 151.9, 149.4, 122.3, 119.4, 98.7, 95.6, 49.6; ¹⁹F NMR (282 MHz, Acetone-*d*₆) δ -78.82; HRMS (ESI-TOF) *m/z* calcd for C₁₁H₇Br₂I₂N₂: 578.7060 [M]⁺; found, 578.7038; *m/z* calcd for CF₃O₃S: 148.9526 [M]⁺; found, 148.9510.

3,3'-Dibromo-5,5'-diiodo-1-octyl-[4,4'-bipyridin]-1-ium trifluoromethanesulfonate (12c). Starting from bipyridine **11** (100 mg, 0.18 mmol) and *n*-octyltriflate (47 mg, 0.18 mmol). 137 mg, yield: 92%. White solid, mp 156-160 °C; ¹H NMR (300 MHz, Acetone-*d*₆) δ 9.93 (d, *J* = 1.3 Hz, 1H), 9.87 (d, *J* = 1.3 Hz, 1H), 9.20 (s, 1H), 9.02 (s, 1H), 5.02-4.93 (m, 2H), 2.36-2.20 (m, 2H), 1.52-1.25 (m, 10H), 0.95-0.79 (m, 3H); ¹³C NMR (126 MHz, Acetone-*d*₆) δ 160.9, 156.7, 152.2, 151.6, 151.0, 147.6, 122.1, 118.4, 98.5, 94.9, 62.8, 31.6, 31.0, 28.9, 28.8, 25.9, 22.4, 13.5; ¹⁹F NMR (282 MHz, Acetone-*d*₆) δ -78.79; HRMS (ESI-TOF) *m/z* calcd for C₁₈H₂₁Br₂I₂N₂: 676.8155 [M]⁺; found, 676.8155; *m/z* calcd for CF₃O₃S: 148.9526 [M]⁺; found, 148.9527.

General procedure for the synthesis of 15a,b, 16 and 17. Bipyridine **11**, **13** or **14** (1 eq.) was solubilized in CH₃CN (2 mL) and placed in a tube equipped with a magnetic stir bar. The electrophile (*n*-octyl iodide or *n*-octyl triflate) was added (3 eq.) and the tube was sealed with a screw cap. The mixture was stirred for 24 h at 120 °C. After cooling to room temperature, the mixture was filtrated and washed with Et₂O (2 x 5 mL) and dried under vacuum overnight to give the desired product.

1,1'-Dioctyl-[4,4'-bipyridine]-1,1'-diium bis(iodide) (15a).^[39] Starting from 4,4'-bipyridine (0.2 g, 1.3 mmol) and *n*-octyl iodide (0.63 g, 2.6 mmol). 0.82 g, yield: 99%. White solid. ¹H NMR (500 MHz, CD₃OD) δ 9.30 (d, *J* = 6.9 Hz, 3H), 8.70 (d, *J* = 6.3 Hz, 4H), 4.76 (t, *J* = 7.6 Hz, 4H), 2.10 (q, *J* = 7.6 Hz, 4H), 1.54 - 1.21 (m, 20H), 0.91 (t, *J* = 6.7 Hz, 6H); ¹³C NMR (126 MHz, CD₃OD) δ 151.3, 147.1, 128.4, 63.3, 32.9, 32.6, 30.2, 30.1, 27.3, 23.7, 14.4.

1,1'-Dioctyl-[4,4'-bipyridine]-1,1'-diium bis(trifluoromethanesulfonate) (15b). Starting from 4,4'-bipyridine (0.2 g, 1.3 mmol) and *n*-octyl triflate (0.63 g, 2.6 mmol). 0.87 g, yield: 98%. ¹H NMR (500 MHz, DMSO-*d*₆) δ 9.36 (d, *J* = 6.5 Hz, 4H), 8.76 (d, *J* = 6.4 Hz, 4H), 4.67 (t, *J* = 7.4 Hz, 4H), 1.97 (t, *J* = 7.1 Hz, 4H), 1.40 - 1.20 (m, 20H), 0.95-0.76 (m, 6H); ¹³C NMR (126 MHz, DMSO-*d*₆) δ 148.7, 145.8, 126.7, 120.7 (q, *J* = 322.3 Hz), 61.0, 31.2, 30.8, 28.5, 28.4, 25.5, 22.1, 14.0; ¹⁹F NMR (471 MHz, DMSO-*d*₆) δ -77.8. HRMS (ESI-TOF) *m/z* calcd for C₂₆H₄₂N₂: 191.1669 [M]²⁺; found, 191.1666; *m/z* calcd for CF₃O₃S: 148.9526 [M]⁺; found, 148.9526.

3,3',5,5'-Tetramethyl-1,1'-dioctyl-[4,4'-bipyridin]-1-diium bis(trifluoromethanesulfonate) (16). Starting from

3,3',5,5'-tetramethyl-4,4'-bipyridine (143 mg, 0.67 mmol) and *n*-octyl iodide (441 mg, 1.7 mmol). 0.49 g, yield: 99%. White solid, mp 168–171 °C; ¹H NMR (500 MHz, Acetone-*d*6) δ 9.21 (s, 4H), 4.86–4.74 (m, 4H), 2.28 (d, *J* = 0.7 Hz, 12H), 2.22–2.14 (m, 4H), 1.54–1.45 (m, 4H), 1.45–1.36 (m, 4H), 1.36–1.22 (m, 12H), 0.87 (t, *J* = 6.9 Hz, 6H); ¹³C NMR (126 MHz, Acetone-*d*6) δ 151.7, 144.8, 137.5, 66.1, 62.8, 32.5, 32.0, 26.8, 23.3, 17.0, 15.6, 14.3; ¹⁹F NMR (471 MHz, Acetone-*d*6) δ -78.89; HRMS (ESI-TOF) *m/z* calcd for C₃₀H₅₀N₂: 219.1981 [M]²⁺; found, 219.1978; *m/z* calcd for CF₃O₃S: 148.9526 [M]⁺; found, 148.9510.

3,3'-Dibromo-5,5'-diiodo-1,1'-dioctyl-[4,4'-bipyridine]-1,1'-dium bis(trifluoromethanesulfonate) (17). Starting from bipyridine **11** (54 mg, 0.10 mmol) *n*-octyltriflate (100 mg, 0.38 mmol). 60 mg, yield: 58%. White solid, mp 197–200 °C; ¹H NMR (500 MHz, Acetone-*d*6) δ 9.99 (s, 2H), 9.93 (s, 2H), 5.03–4.93 (m, 4H), 2.35–2.23 (m, 4H), 1.55–1.49 (m, 4H), 1.45–1.37 (m, 4H), 1.37–1.23 (m, 12H), 0.90–0.82 (m, 6H); ¹³C NMR (126 MHz, Acetone-*d*6) δ 159.8, 153.5, 148.7, 122.2 (q, *J* = 321.5 Hz), 122.1, 63.9, 32.4, 32.0, 29.7, 29.7, 26.8, 23.3, 14.3; ¹⁹F NMR (282 MHz, Acetone-*d*6) δ -78.84; HRMS (ESI-TOF) [M]⁺ *m/z* calcd for C₂₆H₃₈Br₂I₂N₂: 578.7060 [M]⁺; found, 578.7032.

General procedure for the synthesis of imines 19.^[40] A mixture of MgSO₄ (1 g) in DCM (10 mL) was stirred for 10 minutes at room temperature. The relevant aldehyde (10 mmol, 1 eq.) and amine (10 mmol, 1 eq.) were sequentially added. The reaction was stirred under argon for 18 h. The mixture was diluted with DCM and then filtered. The filtrate was concentrated to give crude imine which was used without further purification. Purity > 95% was evidenced by ¹H NMR for all imines.

General procedure for the aza Diels-Alder reaction. In a round-bottom flask under argon at 25 °C, the imine (0.5 mmol) was diluted in dry CH₂Cl₂ (2.5 mL) and *trans*-1-methoxy-3-trimethylsiloxy-1,3-butadiene **18** was added. The catalyst (0.025 mmol) diluted in dry dichloromethane (0.5 mL) was added and the mixture was stirred for 1h. The reaction was quenched by addition of 1 mL of TBAF (1.0 M in THF) and the mixture was stirred for 15 min. Water (10 mL) was added and the phases were separated. The aqueous phase was extracted with CH₂Cl₂ (3 x 15 mL) then the organic phases were combined and dried over MgSO₄. After filtration and concentration, the crude was purified by chromatography on silica gel (cyclohexane / ethyl acetate mixture) to give pure product.

1,2-Diphenyl-2,3-dihydropyridin-4(1H)-one (20a).^[41] Yellow solid; 118 mg (95%) with **15b** and 116 mg (93%) with **12c**. ¹H NMR (500 MHz, CDCl₃) δ 7.68 (dd, *J* = 8.0, 1.4 Hz, 1H), 7.38–7.20 (m, 5H), 7.11 (t, *J* = 7.3 Hz, 1H), 7.02 (d, *J* = 8.7, 2H), 5.33–5.24 (m, 2H), 3.31 (dd, *J* = 16.4, 7.2 Hz, 1H), 2.79 (ddd, *J* = 16.4, 3.1, 1.2 Hz, 1H); ¹³C{¹H} NMR (126 MHz, CDCl₃) δ 190.4, 148.3, 144.8, 138.0, 129.7, 129.1, 128.0, 126.3, 124.5, 118.6, 103.2, 61.8, 43.6.

1-Phenyl-2-(*p*-tolyl)-2,3-dihydropyridin-4(1H)-one (20b).^[41] Yellow solid; 122 mg (93%) with **15b** and 118 mg (90%) with **12c**. ¹H NMR (500 MHz, CDCl₃) δ 7.67 (dd, *J* = 7.8, 1.2 Hz, 1H), 7.30 (dd, *J* = 8.7, 7.5 Hz, 2H), 7.17–7.08 (m, 5H), 7.03 (dd, *J* = 8.7, 1.2 Hz, 2H), 5.31–5.23 (m, 2H), 3.28 (dd, *J* = 16.3, 7.0 Hz, 1H), 2.77 (ddd, *J* = 16.3, 3.4, 1.2 Hz, 1H), 2.31 (s, 3H); ¹³C{¹H} NMR (126 MHz, CDCl₃) δ 190.5, 148.3, 144.9, 133.7, 134.9, 129.8, 129.7, 126.2, 124.5, 118.6, 61.6, 43.7, 27.0, 21.2.

2-(4-Nitrophenyl)-1-phenyl-2,3-dihydropyridin-4(1H)-one (20c).^[41] Yellow solid; 104 mg (71%) with **15b** and 111 mg (76%) with **12c**. ¹H NMR (500 MHz, CDCl₃) δ 8.20 (d, *J* = 8.9 Hz, 2H), 7.71 (d, *J* = 8.0 Hz, 1H), 7.47 (d, *J* = 8.9 Hz, 2H), 7.32 (t, *J* = 7.7 Hz, 2H), 7.15 (t, *J* = 7.5 Hz, 1H), 6.98 (d, *J* = 7.6 Hz, 2H), 5.42–5.36 (m, 1H), 5.33 (d, *J* = 8.0 Hz, 1H), 3.36 (dd, *J* = 16.6, 7.3 Hz, 1H), 2.78 (dd, *J* = 16.6, 2.0 Hz, 1H); ¹³C{¹H} NMR (126 MHz, CDCl₃) δ

189.3, 148.2, 147.8, 145.6, 144.3, 130.0, 127.4, 125.1, 124.5, 118.6, 103.7, 61.4, 43.1.

2-(2-Methoxyphenyl)-1-phenyl-2,3-dihydropyridin-4(1H)-one (20d). Yellow solid; 91 mg (65%) with **15b** and 127 mg (91%) with **12c**. ¹H NMR (500 MHz, CDCl₃) δ 7.75 (dd, *J* = 7.8, 1.4 Hz, 1H), 7.30–7.22 (m, 3H), 7.18 (dd, *J* = 7.7, 1.9 Hz, 2H), 7.08 (t, *J* = 7.5 Hz, 1H), 6.98 (d, *J* = 7.7 Hz, 2H), 6.93 (dd, *J* = 8.3, 1.1 Hz, 1H), 6.84 (dt, *J* = 7.5, 1.1 Hz, 1H), 5.60 (d, *J* = 7.1 Hz, 1H), 5.27 (dd, *J* = 7.8, 1.2 Hz, 1H), 3.87 (s, 3H), 3.20 (dd, *J* = 16.7, 7.7 Hz, 1H), 2.85 (ddd, *J* = 16.7, 2.6, 1.2 Hz, 1H); ¹³C{¹H} NMR (126 MHz, CDCl₃) δ 191.5, 156.1, 148.6, 144.7, 129.6, 129.2, 126.9, 125.0, 124.2, 120.6, 118.1, 111.1, 102.5, 57.0, 55.4, 41.2. HRMS (ESI-TOF) *m/z* calcd for C₁₈H₁₈NO₂: 280.1332 [M]⁺; found, 280.1314.

2-(3-Methoxyphenyl)-1-phenyl-2,3-dihydropyridin-4(1H)-one (20e). Yellow solid; 85 mg (61%) with **15b** and 100 mg (72%) with **12c**. ¹H NMR (500 MHz, CDCl₃) δ 7.67 (dd, *J* = 7.8, 1.2 Hz, 1H), 7.30–7.22 (m, 3H), 7.11 (t, *J* = 7.5 Hz, 1H), 7.03 (d, *J* = 7.7 Hz, 1H), 6.86 (d, *J* = 7.8 Hz, 1H), 6.82–6.77 (m, 2H), 5.29 (d, *J* = 7.7 Hz, 1H), 5.24 (dd, *J* = 7.3, 2.9 Hz, 1H), 3.76 (s, 3H), 3.30 (dd, *J* = 16.3, 7.2 Hz, 1H), 2.78 (ddd, *J* = 16.3, 3.1, 1.2 Hz, 1H); ¹³C{¹H} NMR (126 MHz, CDCl₃) δ 190.4, 160.1, 148.3, 144.8, 139.8, 130.3, 129.7, 124.5, 118.6, 118.5, 112.8, 112.5, 103.1, 61.8, 55.4, 43.6. HRMS (ESI-TOF) *m/z* calcd for C₁₈H₁₈NO₂: 280.1332 [M]⁺; found, 280.1312.

2-(4-Methoxyphenyl)-1-phenyl-2,3-dihydropyridin-4(1H)-one (20f).^[30] Yellow solid; 119 mg (85%) with **15b** and 114 mg (82%) with **12c**. ¹H NMR (500 MHz, CDCl₃) δ 7.65 (dd, *J* = 7.8, 1.2 Hz, 1H), 7.30 (dd, *J* = 8.7, 7.3 Hz, 2H), 7.18 (d, *J* = 8.9 Hz, 2H), 7.11 (t, *J* = 7.3 Hz, 1H), 7.03 (d, *J* = 7.8 Hz, 2H), 6.85 (d, *J* = 8.7 Hz, 2H), 5.28 (dq, *J* = 6.4, 1.2 Hz, 1H), 5.24 (dd, *J* = 6.4, 3.4 Hz, 1H), 3.78 (s, 3H), 3.27 (dd, *J* = 16.3, 7.0 Hz, 1H), 2.76 (ddd, *J* = 16.3, 3.4, 1.2 Hz, 1H); ¹³C{¹H} NMR (126 MHz, CDCl₃) δ 190.6, 159.3, 148.3, 144.9, 129.9, 129.7, 127.5, 124.5, 118.8, 114.5, 61.4, 55.4, 43.8.

2-(4-Dimethylaminophenyl)-1-phenyl-2,3-dihydropyridin-4(1H)-one (20g). Yellow solid; 102 mg (70%) with **15b**. ¹H NMR (500 MHz, CDCl₃) δ 7.63 (dd, *J* = 7.8, 1.2 Hz, 1H), 7.29 (dd, *J* = 8.8, 7.5 Hz, 2H), 7.14–7.07 (m, 3H), 7.05 (d, *J* = 7.6 Hz, 2H), 6.65 (d, *J* = 8.9 Hz, 2H), 5.26 (dd, *J* = 7.8, 1.2 Hz, 1H), 5.21 (dd, *J* = 6.9, 3.5 Hz, 1H), 3.24 (dd, *J* = 16.4, 6.9 Hz, 1H), 2.92 (s, 6H), 2.76 (ddd, *J* = 16.4, 3.4, 1.4 Hz, 1H); ¹³C{¹H} NMR (126 MHz, CDCl₃) δ 191.0, 150.2, 148.3, 145.1, 129.6, 127.1, 125.2, 124.4, 118.8, 112.8, 102.8, 61.5, 43.8, 40.6. HRMS (ESI-TOF) *m/z* calcd for C₁₉H₂₁N₂O: 293.1648 [M]⁺; found, 293.1632.

1-(4-Methoxyphenyl)-2-(*p*-tolyl)-2,3-dihydropyridin-4(1H)-one (20h).^[42] Yellow solid; 123 mg (84%) with **12c**. ¹H NMR (500 MHz, CDCl₃) δ 7.52 (dd, *J* = 7.8, 1.1 Hz, 1H), 7.14 (d, *J* = 8.3 Hz, 2H), 7.10 (d, *J* = 8.3 Hz, 2H), 6.95 (d, *J* = 9.0 Hz, 2H), 6.80 (d, *J* = 9.0 Hz, 2H), 5.21 (dd, *J* = 7.8, 1.2 Hz, 1H), 5.15 (dd, *J* = 7.2, 3.8 Hz, 1H), 3.75 (s, 3H), 3.23 (dd, *J* = 16.4, 7.2 Hz, 1H), 2.74 (ddd, *J* = 16.4, 3.8, 1.2 Hz, 1H), 2.30 (s, 3H); ¹³C{¹H} NMR (126 MHz, CDCl₃) δ 190.4, 156.9, 149.6, 138.5, 137.7, 135.3, 129.7, 126.3, 121.1, 114.7, 101.7, 62.3, 55.6, 43.7, 21.1.

1-(4-Fluorophenyl)-2-(4-methoxyphenyl)-2,3-dihydropyridin-4(1H)-one (20i). Yellow solid; 137 mg (92%) with **15a** and 132 mg (89%) with **12c**. ¹H NMR (500 MHz, CDCl₃) δ 7.51 (dd, *J* = 8.1, 1.1 Hz, 1H), 7.16 (d, *J* = 8.3 Hz, 2H), 7.01–6.94 (m, 4H), 6.83 (d, *J* = 8.8 Hz, 2H), 5.25 (dd, *J* = 7.8, 1.2 Hz, 1H), 5.15 (dd, *J* = 7.2, 3.8 Hz, 1H), 3.77 (s, 3H), 3.21 (dd, *J* = 16.4, 7.2 Hz, 1H), 2.75 (ddd, *J* = 16.4, 3.8, 1.2 Hz, 1H), 2.30 (s, 3H); ¹³C{¹H} NMR (126 MHz, CDCl₃) δ 190.5, 159.9 (d, *J*_{C-F} = 245 Hz), 159.4, 149.1, 141.3, 129.9, 121.3 (d, *J*_{C-F} = 8.2 Hz), 116.4 (d, *J*_{C-F} = 22.8 Hz), 114.5, 102.6, 62.1, 55.4, 43.9. ¹⁹F NMR (282 MHz,

CDCl₃) δ -117.6. HRMS (ESI-TOF) m/z calcd for C₁₈H₁₇FNO₂: 298.1238 [M]⁺; found, 298.1222.

Acknowledgements

This research was funded by the International Center Frontier Research in Chemistry (icFRC), the LabEx CSC (ANR-10-LABX-0026 CSC). RB thanks the LabEx CSC, Strasbourg, for a PhD fellowship.

References

- [1] S. Sowmiah, J. M. S. S. Esperança, L. P. N. Rebelo, C. A. M. Afonso, *Org. Chem. Front.* **2018**, *5*, 453–493.
- [2] Y. Yang, A. A. Sauve, *Biochim. Biophys. Acta Proteins Proteom.* **2016**, *1864*, 1787–1800.
- [3] a) K. Sepčić, *J. Toxicol. Toxin Rev.* **2000**, *19*, 139–160; b) C. Timm, T. Mordhorst, M. Kock, *Mar. Drugs*, **2010**, *8*, 483–497.
- [4] a) S. L. Rössler, B. J. Jelier, E. Magnier, G. Dagousset, E. M. Carreira, A. Togni, *Angew. Chem. Int. Ed.* **2020**, *59*, 9264–9280; b) F.-S. He, S. Ye, J. Wu, *ACS Catal.* **2019**, *9*, 8943–8960.
- [5] D. J. Brunelle, D. A. Singleton, *Tetrahedron Lett.* **1984**, *25*, 3383–3386.
- [6] T. Welton, *Chem. Rev.* **1999**, *99*, 2071–2084.
- [7] a) J. M. J. Nolsøe, M. Aursnes, J. E. Tungen, T. V. Hansen, *J. Org. Chem.* **2015**, *80*, 5377–5385; b) A. M. Kearney, C. D. Vanderwal, *Angew. Chem. Int. Ed.* **2006**, *45*, 7803–7806; c) K. G. Primdahl, J. M. J. Nolsøe, M. Aursnes *Org. Biomol. Chem.* **2020**, *18*, 9050–9059.
- [8] V. Mamane, *Curr. Org. Chem.* **2017**, *21*, 1342–1392.
- [9] T. Damiano, D. Morton, A. Nelson, *Org. Biomol. Chem.* **2007**, *5*, 2735–2752.
- [10] M. C. Grenier, R. W. Davis, K. L. Wilson-Henjum, J. E. LaDow, J. W. Black, K. L. Caran, K. Seifert, K. P. C. Minbiole, *Bioorg. Med. Chem. Lett.* **2012**, *22*, 4055–4058.
- [11] L. Striepe, T. Baumgartner, *Chem. Eur. J.* **2017**, *23*, 16924–16940.
- [12] A. Berkessel, S. Das, D. Pekel, J.-M. Neudörfl, *Angew. Chem.* **2014**, *126*, 11846–11850; *Angew. Chem. Int. Ed.* **2014**, *53*, 11660–11664.
- [13] P. Nagorny, Z. Sun, *Beilstein J. Org. Chem.* **2016**, *12*, 2834–2848.
- [14] C. Thomas, A. Milet, F. Peruch, B. Bibal, *Polym. Chem.* **2013**, *4*, 3491–3498.
- [15] C. Thomas, S. Brut, B. Bibal, *Tetrahedron* **2014**, *70*, 1646–1650.
- [16] B. Procuranti, S. J. Connon, *Org. Lett.* **2008**, *10*, 4935–4938.
- [17] S. Das, D. Pekel, J.-M. Neudörfl, A. Berkessel, *Angew. Chem.* **2015**, *127*, 12656–12660; *Angew. Chem. Int. Ed.* **2015**, *54*, 12479–12483.
- [18] a) R. Sutar, S. M. Huber, *ACS Catal.* **2019**, *9*, 9622–9639; b) J. Bamberger, F. Ostler, O. Garcia Mancheño, *ChemCatChem* **2019**, *11*, 5198–5211.
- [19] P. Politzer, J. S. Murray, T. Clark, *Phys. Chem. Chem. Phys.* **2013**, *15*, 11178–11189.
- [20] a) K. Raatikainen, M. Cametti, K. Rissanen, *Beilstein J. Org. Chem.* **2010**, *6*, No. 4; b) J. E. Ormond-Prout, P. Smart, L. Brammer, *Cryst. Growth Des.* **2012**, *12*, 205–216; c) Y. Kosaka, H. M. Yamamoto, A. Tajima, A. Nakao, H. Cuia, R. Kato, *CrystEngComm* **2013**, *15*, 3200–3211; d) C. J. Kassl, D. C. Swenson, F. C. Pigge, *Cryst. Growth Des.* **2015**, *15*, 4571–4580; e) V. Amendola, G. Bergamaschi, M. Boiocchi, N. Fusco, M. V. La Rocca, L. Linati, E. Lo Presti, M. Mella, P. Metrangolo, A. Miljkovic, *RSC Adv.* **2016**, *6*, 67540–67549; f) A. Dreger, E. Engelage, B. Mallick, P. D. Beer, S. M. Huber, *Chem. Commun.* **2018**, *54*, 4013–4016.
- [21] F. Kniep, S. M. Walter, E. Herdtweck, S. M. Huber, *Chem. Eur. J.* **2012**, *18*, 1306–1310.
- [22] Y.-C. Chan, Y.-Y. Yeung, *Angew. Chem.* **2018**, *130*, 3541–3545; *Angew. Chem. Int. Ed.* **2018**, *57*, 3483–3487.
- [23] H. Zhang, P. H. Toy, *Adv. Synth. Catal.* **2021**, *363*, 215–221.
- [24] P. E. Reyes-Gutiérrez, T. T. Amatov, P. Švec, I. Čísařová, D. Šaman, R. Pohl, F. Teplý, L. Pospíšil, *ChemPlusChem* **2020**, *85*, 2212–2218.
- [25] a) Z. Xue, A. Mazumdar, L. J. Hope-Weeks, M. F. Mayer, *Tetrahedron Lett.* **2008**, *49*, 4601–4603; b) Z. Xue, A. Samanta, B. R. Whittlesey, M. F. Mayer, *Tetrahedron Lett.* **2009**, *50*, 6064–6067.
- [26] a) R. Weiss, E. Aubert, P. Peluso, S. Cossu, P. Pale, V. Mamane, *Molecules* **2019**, *24*, 4484; b) V. Mamane, P. Peluso, E. Aubert, R. Weiss, E. Wenger, S. Cossu, P. Pale, *Organometallics* **2020**, *39*, 3936–3950; c) R. Weiss, E. Aubert, P. Pale, V. Mamane, *Angew. Chem. Int. Ed.* **2021**, *10.1002/anie.202105482*.
- [27] G. Blond, M. Gulea, V. Mamane, *Curr. Org. Chem.* **2016**, *20*, 2161–2210.
- [28] a) Y. Park, E. Park, H. Jung, Y.-J. Lee, S.-s. Jew, H.-g. Park, *Tetrahedron* **2011**, *67*, 1166–1170; b) Y. Kumatabara, S. Kaneko, S. Nakata, S. Shirakawa, K. Maruoka, *Chem. Asian J.* **2016**, *11*, 2126–2129; c) M. Yamanaka, A. Mochizuki, T. Nakamura, K. Maruoka, S. Shirakawa, *Heterocycles* **2020**, *101*, 580–592.
- [29] S. Kaneko, Y. Kumatabara, S. Shimizu, K. Maruoka, S. Shirakawa, *Chem. Commun.* **2017**, *53*, 119–122.
- [30] a) M. Kaasik, A. Metsala, S. Kaabel, K. Kriis, I. Järving, T. Kanger, *J. Org. Chem.* **2019**, *84*, 4294–4303; b) Y. Takeda, D. Hisakuni, C.-H. Lin, S. Minakata, *Org. Lett.* **2015**, *17*, 318–321.

- [31] C. Q. He, C. C. Lam, P. Yu, Z. Song, M. Chen, Y.-h. Lam, S. Chen, K. N. Houk, *J. Org. Chem.* **2020**, *85*, 2618–2625.
- [32] V. Mamane, E. Aubert, P. Peluso, S. Cossu, *J. Org. Chem.* **2012**, *77*, 2579–2583.
- [33] A. Rang, M. Engeser, N. M. Maier, M. Nieger, W. Lindner, C. A. Schalley, *Chem. Eur. J.* **2008**, *14*, 3855–3859.
- [34] a) F. Kniep, S. H. Jungbauer, Q. Zhang, S. M. Walter, S. Schindler, I. Schnapperelle, E. Herdweck, S. M. Huber, *Angew. Chem., Int. Ed.* **2013**, *52*, 7028–7032; b) For a review on halogen bonding anion recognition, see: A. Brown, P. D. Beer, *Chem. Commun.* **2016**, *52*, 8645–8658.
- [35] a) C. Y. Legault, CYLview, 1.0b; University of Sherbrooke, 2009 (<http://www.cylview.org>); b) CCDC 2095512 (**12a**) and 2095511 (**12b**) contain the supplementary crystallographic data for this paper. These data are provided free of charge by The Cambridge Crystallographic Data Centre.
- [36] A.-C. C. Carlsson, J. Gräfenstein, A. Budnjo, J. L. Laurila, J. Bergquist, A. Karim, R. Kleinmaier, U. Brath, M. Erdélyi, *J. Am. Chem. Soc.* **2012**, *134*, 5706–5715.
- [37] J. Šturala, S. Boháčová, J. Chudoba, R. Metelková, R. Cibulka, *J. Org. Chem.* **2015**, *80*, 2676–2699.
- [38] C. M. Timperley, M. Bird, S. C. Heard, S. Notman, R. W. Read, J. E. H. Tattersall, S. R. Turner, *J. Fluorine Chem.* **2005**, *126*, 1160–1165.
- [39] M. Rueping, P. Nikolaienko, Y. Lebedev, A. Adams, *Green Chem.* **2017**, *19*, 2571–2575.
- [40] P. J. Alaimo, R. O'Brien III, A. W. Johnson, S. R. Slauson, J. M. O'Brien, E. L. Tyson, A.-L. Marshall, C. E. Ottinger, J. G. Chacon, L. Wallace, C. Y. Paulino, S. Connell, *Org. Lett.* **2008**, *10*, 5111–5114.
- [41] J. A. Leitch, T. Rogova, F. Duarte, D. J. Dixon, *Angew. Chem. Int. Ed.* **2020**, *59*, 4121–4130.
- [42] F. Bellezza, A. Cipiciani, U. Costantino, F. Fringuelli, M. Orrù, O. Piermatti, F. Pizzo, *Catal. Today* **2010**, *152*, 61–65.

